The Nitrate Transporting Photochemical Reaction Cycle of the Pharaonis Halorhodopsin

Zoltán Bálint,* Melinda Lakatos,* Constanta Ganea,† Janos K. Lanyi,‡ and György Váró*
*Institute of Biophysics, Biological Research Center of the Hungarian Academy of Sciences, Szeged, H-6701, Hungary; †Department of Biophysics, University of Medicine "Carol Davila", 76241 Bucharest, Romania; and ‡Department of Physiology and Biophysics, University of California, Irvine, California USA

ABSTRACT Time-resolved spectroscopy, absorption kinetic and electric signal measurement techniques were used to study the nitrate transporting photocycle of the pharaonis halorhodopsin. The spectral titration reveals two nitrate-binding constants, assigned to two independent binding sites. The high-affinity binding site (K_a = 11 mM) contributes to the appearance of the nitrate transporting photocycle, whereas the low-affinity constant (having a K_a of ~7 M) slows the last decay process in the photocycle. Although the spectra of the intermediates are not the same as those found in the chloride transporting photocycle, the sequence of the intermediates and the energy diagrams are similar. The differences in spectra and energy levels can be attributed to the difference in the size of the transported chloride or nitrate. Electric signal measurements show that a charge is transferred across the membrane during the photocycle, as expected. A new observation is an apparent release and rebinding of a small fraction of the retinal, inside the retinal pocket, during the photocycle. The release occurs during the N-to-O transition, whereas the rebinding happens in several seconds, well after the other steps of the photocycle are over.

INTRODUCTION

Halorhodopsin (HR), an electrogenic light-driven ion pump which belongs to the family of the seven-helical transmembrane proteins, was discovered in the archaea *Halobacterium salinarum* (Matsuno-Yagi and Mukohata, 1977; Lindley and MacDonald, 1979). It is a retinal protein which transports Cl^- from the extracellular side into the cell (Schobert and Lanyi, 1982) and, similarly to the proton pumping bacteriorhodopsin (BR), the translocation is triggered by photoisomerization of the all-*trans* retinal to 13-*cis* form. The chromophore is bound to a lysine via a protonated Schiff base in the same way as in BR.

Since its discovery, various types of HRs have been reported (Otomo et al., 1992; Soppa et al., 1993; Mukohata et al., 1999) but the most extensively studied ones are found in *Halobacterium salinarum* (sHR) and *Natronobacterium pharaonis* (pHR) (Bivin and Stoeckenius, 1986). It was shown that pHR also transports chloride into the cell (Duschl et al., 1990). In contrast with sHR, which in the dark adapted state contains 45% all-*trans* retinal although after light adaptation this content is shifted to a maximum of 75%, in pHR both light- and dark-adapted states contain ~85% all-*trans* retinal (Váró et al., 1995b; Zimányi and Lanyi, 1997) and the 13-*cis* retinal has no measurable photocycle (Váró et al., 1995b).

sHR (Blanck and Oesterhelt, 1987) and pHR show 66% sequence identity (Lanyi et al., 1990). A considerable similarity in the three-dimensional structures was found between HR and BR (Havelka et al., 1995; Kolbe et al., 2000). Several highly conserved amino acids in the binding pocket of retinal, such as Asp-212 in BR (residue 238 in sHR and residue 252 in pHR) and Arg-82 (residue 108 in sHR and residue 123 in pHR), take part in a counterion complex which stabilizes the protonated Schiff base (Needleman et al., 1991; Balashov et al., 1992; Cao et al., 1993).

Resonance Raman spectroscopy studies revealed that the bound chloride in HR is close to the Schiff base (Maeda et al., 1985; Pande et al., 1989) and that it is part of the counterion complex (Ames et al., 1992). A recently published high-resolution (1.8 Å) structure of sHR (Kolbe et al., 2000) showed that chloride takes the place of the proton acceptor in BR, Asp-85. Because it does not function as proton acceptor, however, the Schiff base does not deprotonate in the photocycle. Instead, the mobility of the counterion makes it possible for the anion to follow the change of the orientation of the Schiff base N-H bond from the extracellular to the cytoplasmic side (Oesterhelt et al., 1986). Its motion is the critical step in the transport, changing the specificity of ion translocation from proton to anions. HR can translocate, besides chloride, anions like bromide, iodide, and nitrate with different efficiencies, toward the interior of the cell (Bamberg et al., 1984; Duschl et al., 1990). In the presence of azide the Schiff base deprotonates (Hegemann et al., 1985) and the halide pump is converted into an extracellularly directed proton pump (Váró et al., 1996). Under special conditions, namely in a two-photon excitation, sHR was reported to transport protons in the same direction as chloride (Bamberg et al., 1993).

The photocycle and transport properties of both sHR and pHR have been studied extensively by a variety of techniques. Time resolved ultraviolet-visible spectroscopy allowed the determination of the spectra of the photocycle intermediates (Váró et al., 1995b,c; Chizhov and Engelhard, 2001). The molecular changes during the photocycle could be monitored by infrared difference spectroscopy

Submitted July 22, 2003, and accepted for publication October 30, 2003.

Address reprint requests to György Váró, E-mail: varo@nucleus.szbk.u-szeged.hu.

0006-3495/04/03/1655/09 $2.00

(Rothschild et al., 1988; Braiman et al., 1994; Hackmann et al., 2001) and resonance Raman spectroscopy (Alshuth et al., 1985; Ames et al., 1992; Gerscher et al., 1997). The electric signals from sHR were first measured on membrane fragments adsorbed onto a positively charged planar lipid bilayer (Bamberg et al., 1984). Another method was used for electrical measurements of sHR containing oriented gel samples (Dér et al., 1985a) and, more recently, pHR containing membranes attached to phospholipids-impregnated films (Kalaidzidis et al., 1998). Simultaneous absorption kinetic and electric signal measurements, on oriented gel samples, allowed the calculation of the time courses of the photocycle intermediates and, at the same time, of their electrogenicities (Ludmann et al., 2000). Another attempt to interpret the relation of the electric signals to the photocycle was made by measuring the photocycle in suspension and the electric signals by adsorbing HR containing membranes onto a thin polymer film (Okuno et al., 1999; Muneyuki et al., 2002).

The ionic strength and the presence of the transported anion influence the photocycle of HR. Although different groups use different nomenclatures for the photointermediates and the details of the photocycle are still a matter of debate, it is generally agreed that sHR and pHR have similar photocycles. The sequence of intermediates in the presence of chloride is K, L, N, O, HR′, HR. The main difference between the photocycles of pHR and sHR is that in the latter the O state does not accumulate (Váró et al., 1995c), probably for kinetic reasons. In pHR the release and the uptake of chloride were associated with the N-to-O and O-to-HR′ transitions, respectively (Váró et al., 1995a; Kalaidzidis et al., 1998; Ludmann et al., 2000). Replacement of chloride by sulfate results in nontransporting cycles in both HRs, presumably because the anion-binding site is unoccupied. Without chloride, the absorption maximum of pHR shifted from 578 nm to 600 nm (Scharf and Engelhard, 1994).

It was shown that nitrate can also be transported by sHR, though much less effectively (Zimányi et al., 1989), but pHR transports nitrate as effectively as it does chloride (Duschl et al., 1990). Based on absorption kinetic measurements, the photocycles of pHR in chloride and nitrate seem very similar and in both anions the intermediate absorbing at 640 nm, associated with the O state, could be observed (Scharf and Engelhard, 1994). The equilibrium constants (half-maximal binding) for chloride and nitrate have, at pH 6, values of 1 mM and 16 mM, respectively (Scharf and Engelhard, 1994).

Although several groups described the binding and transport of nitrate by pHR, a detailed kinetic and thermodynamic characterization of its photocycle has been lacking. Therefore, in this study, we report spectral, absorption kinetic, thermodynamic, and electric signal measurements effectuated on gel samples prepared from pHR containing membranes. At low nitrate concentration (up to 200 mM), the earlier described binding constant of the nitrate was confirmed. From spectral and kinetic measurements at high concentrations of nitrate (5 M) an additional binding of nitrate was observed. It was a new and unexpected observation that optical absorption kinetic signals suggested the appearance of free retinal at the end of the photocycle, leading to the conclusion that during the photocycle a small fraction of the cycling HR molecules releases the retinal and later rebinds it.

MATERIALS AND METHODS

Halorhodopsin-containing membrane suspensions were prepared from *Halobacterium salinarum* strain L33, in which the *Natronobacterium pharaonis hop* structural gene and the novobiocin resistance gene for selection were introduced, as described earlier (Váró et al., 1995b). All spectroscopic and absorption kinetic measurements were performed on membranes encased in polyacrylamide gel, as described before (Váró et al., 1995b) on samples of optical density between 0.2 and 0.7 at 570 nm. Electric signal measurements were carried out on oriented gel samples, prepared according to the known procedure (Dér et al., 1985b). Comparative spectroscopic, absorption kinetic, and electric signal measurements did not show any differences between the suspension and gel samples. The advantages of the gel samples were high stability and prevention of aggregation at high salt concentration. Before measurements the samples were exhaustively washed in a solution of 1 M Na_2SO_4, 50 mM MES (2-[*N*-morpholino]ethanesulfonic acid), pH 6. For the measurements the samples were equilibrated with solutions containing 50 mM MES and $NaNO_3$ at different concentrations, prepared in such a way as to keep the sodium ion concentration at the constant value of 2 M, by adding Na_2SO_4. During the measurements the sample was kept in a temperature-controlled sample holder. Flash excitation at 532 nm was performed with a frequency-doubled Nd-YAG laser (Surelite I-10, Continuum, Santa Clara, CA).

Time-resolved spectroscopy with a gated optical multichannel analyzer provided difference spectra at various time points of the photocycle in the 300 ns–100 ms interval (Zimányi and Lanyi, 1989). The spectra of intermediates were calculated from these difference spectra, after noise reduction with singular value decomposition (SVD) (Golub and Kahan, 1992; Váró et al., 1995b; Gergely et al., 1997). For the time-resolved spectral measurements over 100 ms a spectrophotometer card was used (PC2000-ISA, Avantes, Eerbeek, The Netherlands), controlled by a program written in our institute in Labview (version 5.0). After a single laser flash a set of spectra were measured with 10 ms integration time and <40 ms readout of consecutive spectra. In the time interval of 100 ms to 10 s, 15 spectra were recorded at logarithmically equidistant time points.

For absorption kinetic signals a 55-W halogen lamp with a heat filter and monochromator provided the measuring light. The signals were recorded at 500, 590, 620, and 640 nm, in the time interval between 1 μs and 10 s and at six temperatures between 5 and 30°C, using a transient recorder card (NI-DAQ PCI-5102, National Instruments, Austin, TX) with 16 MB memory, controlled by a program, written in our institute in Labview (version 5.0). The signals were fitted with RATE and EYRING programs as described before (Váró et al., 1995a; Ludmann et al., 1998a). The Eyring plots (log k versus $1/T$) were expected to be linear, as during the photocycle of the retinal proteins the heat capacitance of the system does not change (Váró et al., 1995a; Ludmann et al., 1998a).

Each transient spectroscopic and absorption kinetic measurement involved averaging of 100–150 signals. At the end of the measurement, the linear time base was converted to logarithmic by averaging in the time interval between logarithmically equidistant points, which improved the signal-to-noise ratio. In the experiments concerning the free retinal formation and decay, the absorption kinetic signal was recorded at 380 nm and 420 nm with an additional blue filter BG3/4g.

Electric signals were measured on a set-up described previously (Ludmann et al., 1998b), with the modification that a very low-noise

homemade current preamplifier was used. Each electric measurement was effectuated by averaging 600 signals.

RESULTS AND DISCUSSION

Spectral and absorption kinetic titration

The spectra of pHR in the concentration range of 0–5 M nitrate are shown in Fig. 1. The sharp peak at 415 nm corresponds to membrane-bound cytochromes. This peak, being salt concentration independent, allowed normalizing the spectra measured under various conditions, eliminating small amplitude changes originating from salt-dependent volume changes of the gel. Two independent parameters were quantified and presented as a relative change between 0 and 1, between 0 and 500 mM nitrate, respectively. (Note: the range of nitrate shown is >500 mM.) The extent of the blue shift of the spectrum was read from the maximum of the absolute spectra (Fig. 1 *A*) and the amplitude change at 630 nm (Fig. 1 *B*). The spectral titration in the low concentration range of 0–200 mM reveals an apparent binding constant of 11 mM with 0.9 binding order (Fig. 2), confirming the value obtained earlier (Scharf and Engelhard, 1994). This binding

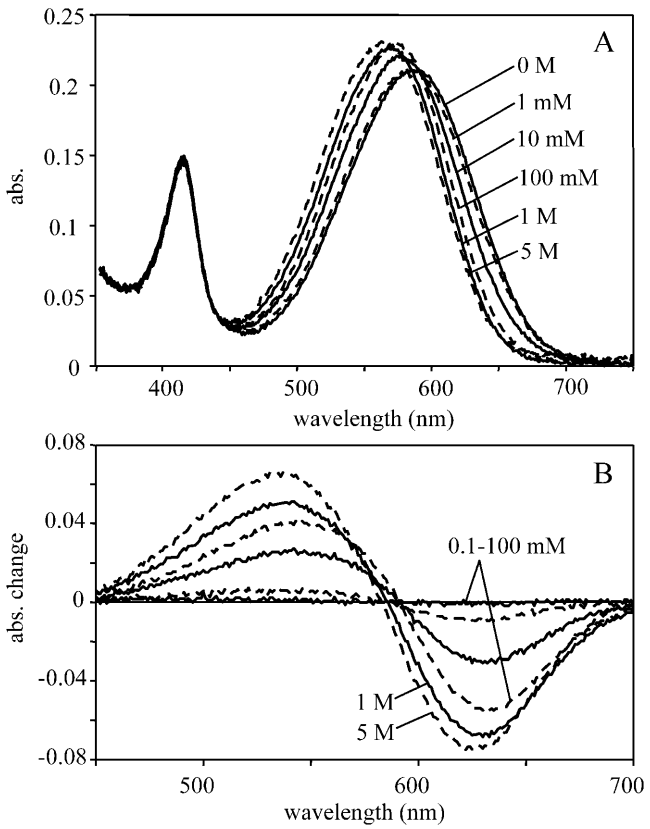

FIGURE 1 Nitrate-dependent changes in the spectrum of the pharaonis halorhodopsin. (*A*) Absorption spectra with an increasing nitrate concentration, by mixing 1 M Na_2SO_4 and 2 M $NaNO_3$. Over 2 M $NaNO_3$ the total Na concentration was increased by using 5 M $NaNO_3$. (*B*) Difference spectra obtained by subtracting the 0 M nitrate spectrum.

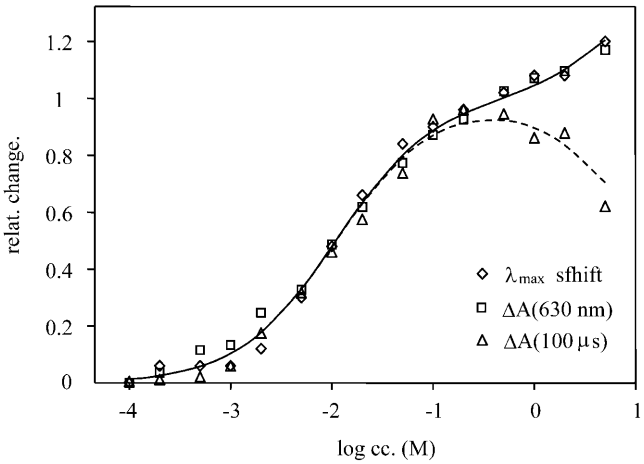

FIGURE 2 Titration curve of the relative spectral shift (◊), the relative amplitude change of the difference spectrum at 630 nm (□), and the relative amplitude change of the 590-nm kinetic signal at 100 μs (△). All the relative changes were normed together at the 10 mM $NaNO_3$ concentration. The kinetic measurements were performed at 200 mM nitrate concentration, where the low-affinity binding site is almost totally saturated.

constant is one order of magnitude larger than for chloride (apparent binding constant 1 mM, with reaction order of 0.75 (Váró et al., 1995b)). The difference spectra in this concentration range have an isosbestic point ~595 nm (Fig. 1 *B*), and show great similarity to those measured in chloride (Váró et al., 1995b). At higher salt concentrations the spectrum shifts further toward blue, revealing the existence of another, low-affinity binding constant estimated at ~7 M. A second low-affinity binding site for halide ions was concluded from photoelectric measurements (Bamberg et al., 1984; Okuno et al., 1999), but the secondary spectral shift was not observed in chloride. This binding site should be on the cytoplasmic side of the membrane, as will be discussed later. The difference between the chloride and nitrate binding is probably due to the size difference between the two ions.

The kinetic signals, measured at selected wavelengths (500, 590, 620, and 640 nm), where the absorption changes are pronounced and differ from each other (Fig. 3), show great similarity to those measured in chloride (Váró et al., 1995a), but the last step of the nitrate photocycle is faster by almost one order of magnitude. The relative amplitude of the largest signal (590 nm), measured at 100 μs, as a function of nitrate concentration was fitted with the same binding constants found at the spectral titration (Fig. 2). The only difference is that whereas in the spectral titration the second nitrate binding contributes by increasing further the relative change, in the kinetic titration it induces a decrease in amplitude. It appears that the second bound nitrate hinders the photocycle. With increasing nitrate concentration above 1 M, all the amplitudes are smaller and the decay of the photocycle becomes slower.

From the titration curve the best condition for an almost totally pure photocycle dominated by the first nitrate-binding

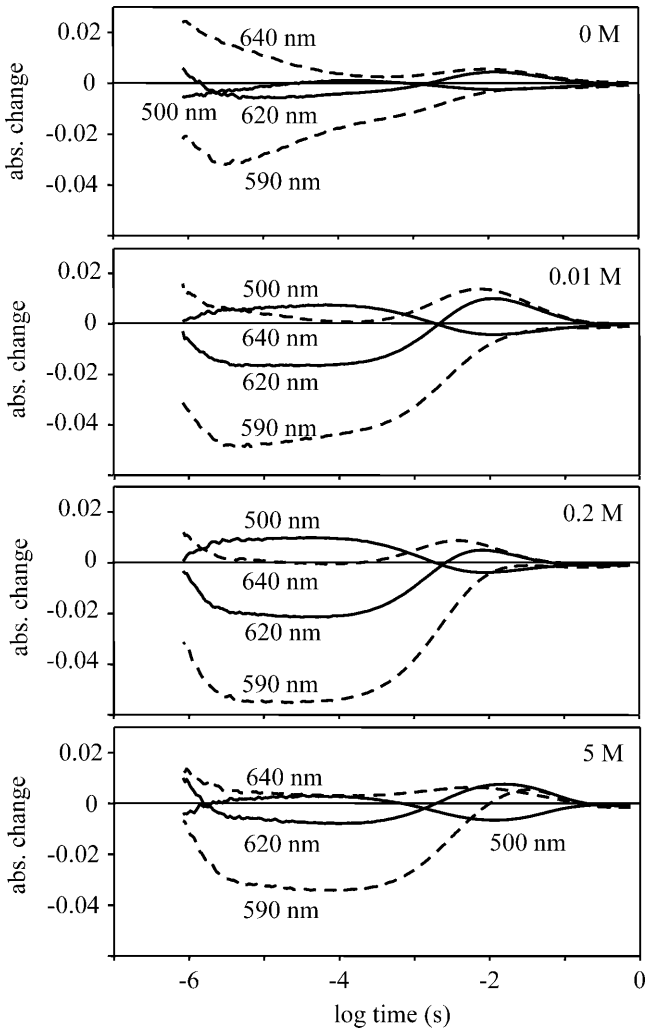

FIGURE 3 Time-dependent absorption kinetic signals measured at various nitrate concentrations. The nitrate concentration was adjusted by mixing 2 M $NaNO_3$ and 1 M Na_2SO_4, to keep the Na^+ concentration at constant 2 M. The solution contained 50 mM MES, at pH 6 and 20°C.

constant, was chosen to be at 200 mM. At this concentration the sulfate photocycle (i.e., the photocycle without a bound anion) is present only in 2–3%, whereas the eventually changed nitrate photocycle, with the second nitrate bound, is present in 3–4% only. In the following study the 200 mM nitrate concentration was considered as the reference point, and we studied it in detail.

The spectra of intermediates

First, the spectra of intermediates were determined with time-resolved optical multichannel spectroscopy. The method of the measurements and the process of eliminating the possible artifacts were as described earlier (Váró et al., 2003; Lakatos et al., 2003). A total of 30 difference spectra were measured in the time interval between 300 ns and 100 ms, spaced at logarithmically equidistant time points. During the SVD of the measured difference spectra, the first three basis spectra components had weight factors of 1.8, 0.28, and 0.076 and autocorrelation products of 0.83, 0.686, and 0.037, respectively (Gergely et al., 1997). All the following basis spectra had even smaller weight factors and autocorrelation products. Based on these, the first two spectral components were considered different from the noise. The reconstructed difference spectra, by using these two spectra and the corresponding amplitudes, are shown on Fig. 4. Besides providing very effective noise filtering, this analysis gives the minimum number of spectrally independent intermediates to be at least two. The complex shape of the basis spectra and their amplitude, and the complexity of the absorption kinetic traces suggest the existence of more spectrally independent and spectrally silent components.

Based on the information gathered from the SVD analysis a model independent search for the spectra of intermediates was performed as described earlier (Gergely et al., 1997). Considering only two spectrally independent intermediates, the spectra had two maxima that were grounds for their rejection, whereas calculating with four intermediates, two of the spectra coincided. The number of different intermediate spectra, with a single maximum, was three (Fig. 5 *A*). Comparing these spectra to those calculated in the chloride transport, several differences can be observed (Váró et al., 1995b). There is no spectrum corresponding to intermed-

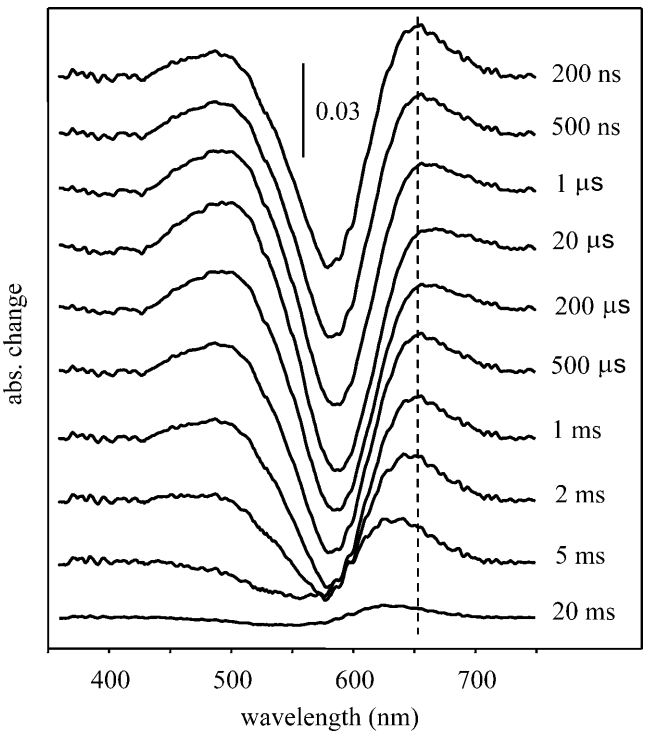

FIGURE 4 SVD-filtered difference spectra of pharaonis halorhodopsin measured at the indicated time delays after laser photoexcitation. Measuring conditions were 200 mM $NaNO_3$, 0.9 M Na_2SO_4, 50 mM MES, pH 6, 20°C. The vertical dotted line helps illustrate the shift of the maximum.

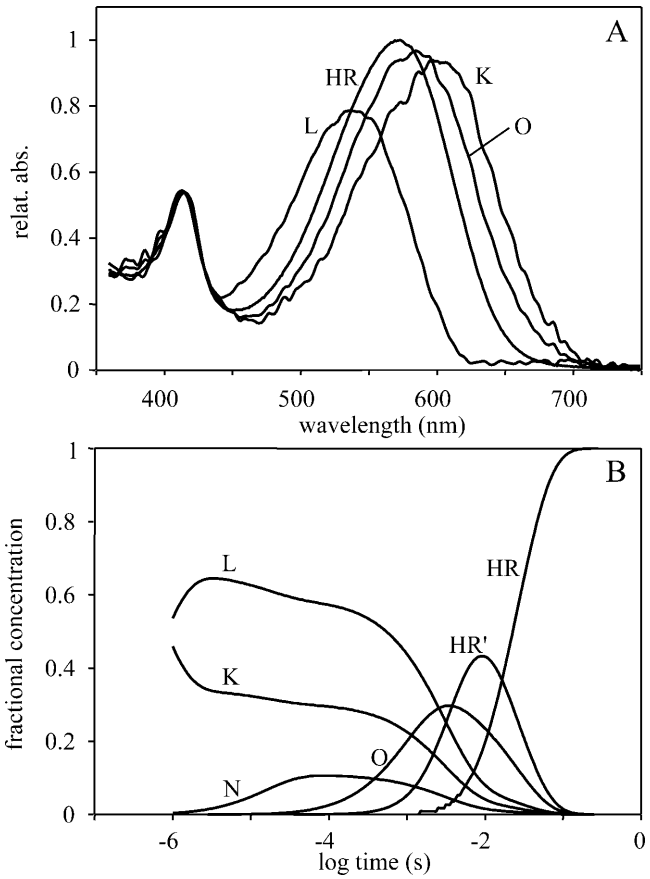

FIGURE 5 Spectra of intermediates (*A*), calculated from the difference spectra in Fig. 4, and the time-dependent concentration changes of intermediates (*B*) calculated from the 200-mM kinetic traces in Fig. 3. The error of the fit was <3%.

iate N. The spectrum of K is red shifted, becoming similar to the K calculated in BR (Gergely et al., 1997), whereas that of O is strongly blue shifted.

Photocycle model

Whereas the kinetic properties of the halorhodopsin at different chloride concentrations were thoroughly studied (Bamberg et al., 1994; Váró et al. 1995a,b; Okuno et al., 1999; Chizhov and Engelhard, 2001), the nitrate transporting photocycle needs to be investigated.

Photocycle at low anion concentration (200 mM)

Using the method developed earlier, different sequential and parallel photocycle models were fitted, with the RATE program, to the absorption kinetic signals measured at six temperatures between 5 and 30°C (Ludmann et al., 1998a; Lakatos et al., 2003). The simplest model, which resulted in a good fit at all temperatures and exhibited linear Eyring plots for all the rate constants (not shown), was the sequential model; similar to that found in the case of chloride transporting pHR:

$$K \Leftrightarrow L \Leftrightarrow N \Leftrightarrow O \Leftrightarrow HR' \Rightarrow HR.$$

In this model the spectrum of L and N was considered similar. We use the notation of N instead of L′, generally used for spectrally silent intermediates, solely to suggest the similarity to the chloride transporting photocycle. The average error of the fit at all temperatures was $<\pm 5\%$. The relative concentration change of the intermediates (Fig. 5 *B*) and the rate constants (Table 1) at 20°C are very similar to those in the case of the chloride transporting photocycle. The prominent accumulation of a long-living L intermediate is the characteristic feature of the photocycle. The main difference between the nitrate- and chloride transporting photocycles is the faster rising and rather long-living intermediate N (Váró et al., 1995b). Based on the Eyring plots the energy diagram of the nitrate cycle was calculated (Fig. 6). Comparing this to the energy diagram of the chloride photocycle, published earlier (Váró et al., 1995a), a change in the energy level of intermediate N is observed. The downshift of the enthalpy level of N is accompanied by a more pronounced upshift of the entropic energy, which results in a slightly raised level of the free energy. This explains the accumulation of intermediate N in a smaller amount in the nitrate photocycle, despite its earlier appearance. The changes in the enthalpy and entropy barriers are mostly found between the L-to-N and, to a smaller extent, between the N-to-O and O-to-HR′ transitions. Probably, the size of the transported ion affects the transitions related to the conformational change of the protein and the ion translocating steps during the photocycle. The volume decrease of the protein observed earlier (Váró et al., 1995a) in the presence of a larger ion can be achieved only by losing some conformation freedom, as observed by the decrease in the entropy of the system (increase in the entropic energy).

Photocycle at high anion concentration (5 M)

In the presence of high halide ion concentration an inhibition of the ion transport was observed in sHR (Bamberg et al., 1984) and pHR (Okuno et al., 1999).

TABLE 1 Rate constants of the nitrate photocycle

Transition	Rate constant
K-to-L	0.7 μs
L-to-K	1.3 μs
L-to-N	89 μs
N-to-L	14 μs
N-to-O	0.77 ms
O-to-N	0.6 ms
O-to-HR′	4.1 ms
HR′-to-O	24.2 ms
HR′-to-HR	38 ms

Rate constants were calculated from the absorption kinetic signals measured at 20°C.

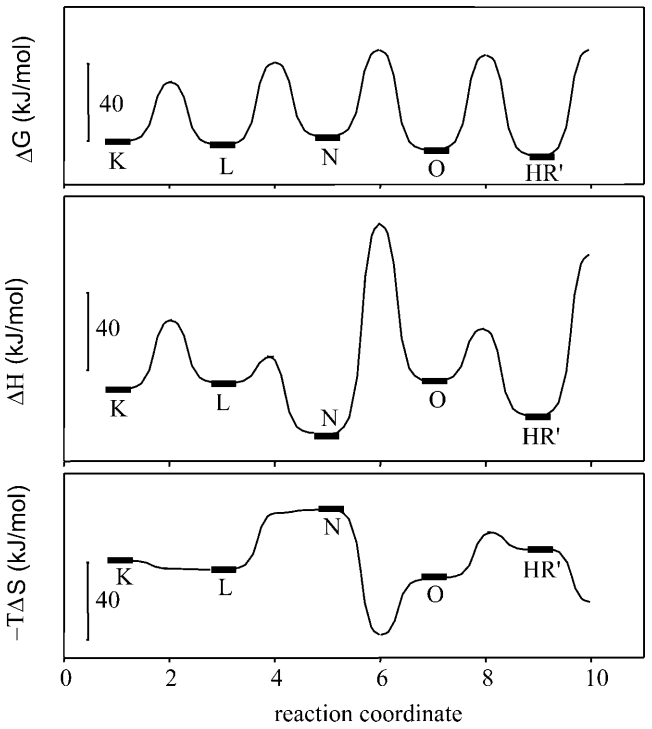

FIGURE 6 Free energy, enthalpy, and entropic energy diagram of the nitrate transporting photocycle of pharaonis halorhodopsin, calculated from the Eyring plots of the rate constants (not shown).

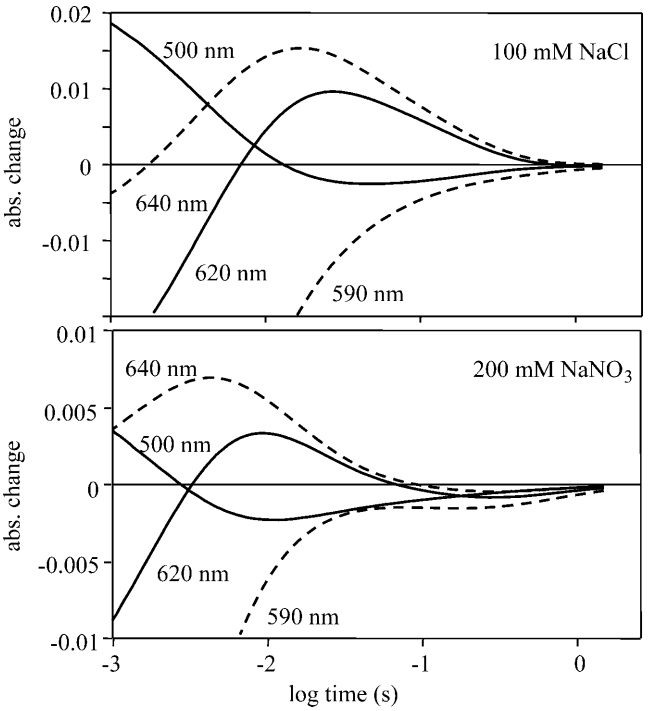

FIGURE 7 Absorption kinetic signals measured in 100 mM NaCl and 200 mM $NaNO_3$. The other measuring conditions were the same as in Fig. 4. Whereas in NaCl all the traces decay smoothly to 0, in $NaNO_3$ there is an extra negative absorbance at each wavelength.

To make only an estimation of the time-dependent concentration change of the pHR photocycle intermediates at 5 M nitrate concentration, all intermediate spectra were shifted ~5 nm toward blue, which is the shift of the pHR spectrum between 200 mM and 5 M nitrate concentration. Without this shift the fit of the photocycle scheme described earlier (for low nitrate) had a lower quality, but the shifted spectra fitted the measurement presented on Fig. 3 (5 M), with ±10% error. The resulting time-dependent concentrations showed a pronounced equilibrium shifted toward the early intermediate K. Fewer L and O intermediates accumulated (not shown). The high nitrate concentration slows the decay of the photocycle, suggesting that the low-affinity binding site could be located on the release side of the membrane, because its saturation hinders the nitrate release. In the halide transporting bacteriorhodopsin mutant D85S a second binding site is observed on the cytoplasmic side of the membrane (Facciotti et al., 2003).

Transient change in the retinal binding

An interesting aspect of the photocycle was observed during the absorption kinetic measurements. Contrary to the signals measured in sulfate and in chloride an extra absorption change was observed at >100 ms time-range in nitrate. At all wavelengths and all nitrate concentrations this absorption change is negative (Figs. 3 and 7). In Fig. 7, the millisecond time range is enlarged for signals measured in chloride and nitrate. Although in chloride the end of the photocycle consists of a smooth decrease of all absorption changes, in the case of nitrate, over 100 ms, these become negative, and go to zero in several seconds. The negative signal at all measured wavelengths suggests that the main absorption peak of the pHR sample decreased. A new, shifted absorption band should appear outside of the observed wavelength range of 400–700 nm.

It is known that the tungsten lamp used has very low intensity below 400 nm. To investigate the spectra in the range of 350–700 nm with similar light intensity and good spectral sensitivity, this interval was divided in two. Between 350 and 450 nm, a blue BG3/4g bandpass filter was used, whereas for the 450 to 700 nm range, a 1 OD (optical density) neutral filter was used, ensuring for the whole interval an almost constant light intensity. The difference spectra in the time period of 100 ms to 10 s show clearly the existence of a positive peak with a maximum at ~375 nm that disappears in time as the negative absorption centered around the main absorption peak of the pHR also decreases (Fig. 8 *A*). The difference spectra show an isosbestic point at ~420 nm, suggesting a simple transition between two states.

The absorption peak of unbound retinal is between 350 and 380 nm, depending on the solvent and retinal configuration (Fisher and Weiss, 1974; Stoeckenius et al., 1979). There is no information about observation of any photocycle

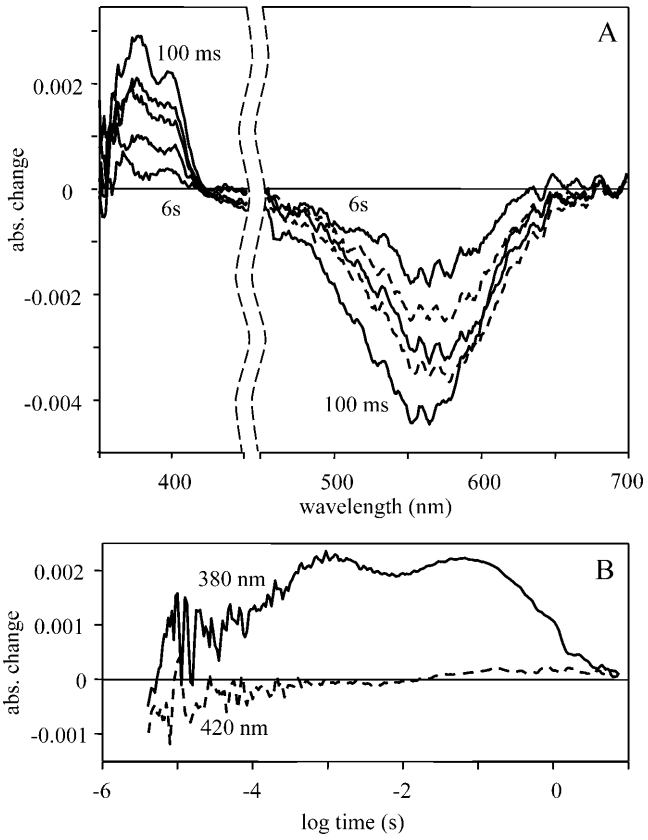

FIGURE 8 Difference spectra (*A*) and absorption kinetic signals (*B*) of the pharaonis halorhodopsin. Measuring conditions were the same as in Fig. 4. The absorption maximum of the difference spectra at 376 nm suggests the existence of the free retinal. The time course of the 380-nm trace shows the release and rebinding of the free retinal during the photocycle.

intermediate in wild-type or mutant ion transporting retinal protein, with a peak below 400 nm, although there is no reason why covalently bound retinal with a deprotonated Schiff base should not absorb there. Although there is no direct evidence that the peak we observe originates from breaking of the covalent bond of the Schiff base, it is probable that in the late part of the photocycle free retinal appears in the binding pocket of the protein. As the retinal is trapped in the binding pocket, it is rebound in the seconds timescale, restoring the ground-state pHR. There are two possibilities for how cleavage of the Schiff base could arise: excitation of the 13-*cis* retinal containing halorhodopsin, which is present even in the light-adapted form (Váró et al., 1995b), or branching of the all-*trans* photocycle. The measured sample had absorption of 0.6 at 560 nm. From the negative amplitude of the difference spectra it can be estimated that ~0.8% of the sample goes through this state, meaning that ~5% from the 13-*cis* retinal containing pHR would participate, if this is the case. From the absorption kinetic signal it can be estimated that ~20–25% of the sample was excited, which results in ~3–4% of the excited part losing its retinal if a branching in the photocycle happens. It is improbable that between the two retinal forms there is such a great quantum efficiency difference, that the same light pulse excites only 5% from the 13-*cis* but 20% from the all-*trans* form, making the branching hypothesis more likely. This is corroborated by the following absorption kinetic measurements.

To get information about the kinetic of appearance and rebinding of the free retinal, the kinetic trace at 380 nm was measured (Fig. 8 *B*). To eliminate the possibility of the absorption changes of the β absorption band of the protein-bound retinal, a control absorption kinetic signal was measured at 420 nm, the isosbestic point observed on the difference spectra (Fig. 8 *A*), taken in the time interval when all the other intermediates had already vanished. Although the absorption change measured at 420 nm remains practically zero, the 380-nm signal has a rise in the 100 μs time range (Fig. 8 *B*) and decays within several seconds. The two peaks of the 380 nm kinetic signal at ~1 ms and 100 ms correlate with the N-to-O and HR′-to-HR transitions of the photocycle (Fig. 5 *B*). These are the transitions when the retinal regains its all-*trans* configuration and the protein relaxes back to its low-energy state. Probably, there are several conformational states of the protein in which these changes—the reisomerization of the retinal and the relaxation process of the protein—affect mostly the Schiff base, breaking the binding of the retinal to the protein. The energy diagram of the photocycle shows in this region a decrease in the entropy. All these observations support the assumption that the free retinal appears as a branching in the photocycle due to a reduced conformational freedom of the protein.

Charge translocation

The electric signal measurements on oriented gel in 200 mM nitrate (Fig. 9, *continuous line*) produced a current signal,

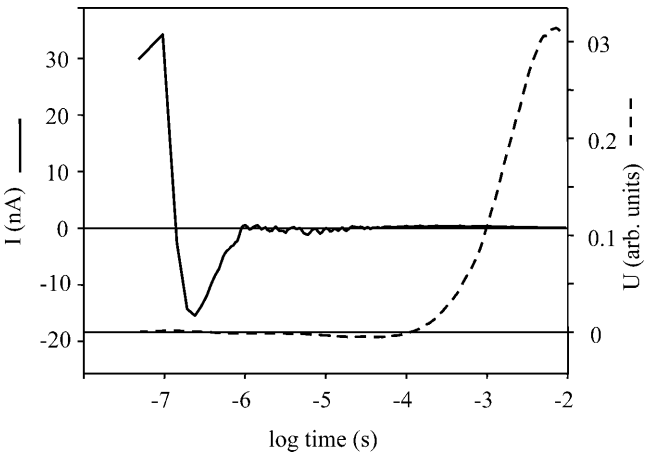

FIGURE 9 Electric current signal measured on an oriented sample of pharaonis halorhodopsin (*continuous line*) and the calculated voltage signal. Measuring conditions were the same as in Fig. 4.

similar to that measured in the case of chloride transport at 10 mM salt concentration (Ludmann et al., 2000). The only difference is the size of the signal in nitrate which is about one order of magnitude smaller. The integral of the signal (Fig. 9, *broken line*) in the millisecond time interval is positive, corroborating that this ion is transported across the membrane. Over 20 ms the electric signal becomes unstable, due to the baseline instability, leaving unresolved the last transition, HR′-to-HR. Based on the analogy to the chloride transporting photocycle, this last step should have also a positive component (Ludmann et al., 2000). Repeating the electric signal measurements several times, the shape of the voltage signal remained the same, but with varying amplitude, presenting the overall tendency of a valid signal, but leaving the possible calculation of the electrogenicity of the intermediates with a large uncertainty.

The above described experiments revealed that the nitrate transporting photocycle of the pHR is very similar to that of the chloride transporting one, but showed the existence of differences in the kinetic properties. The study of the nitrate transporting photocycle of pHR revealed two interesting features:

The existence of a low-affinity binding site, with a binding constant of ~7 M. Based on its effect of slowing the photocycle, the location of the binding site is predicted to be on the cytoplasmic side of the membrane, where the ion release occurs.

Upon reisomerization of the retinal from 13-*cis* to all-*trans* at the end of the photocycle, in a fraction of the excited protein the retinal appears to lose its covalent bond to the protein. The retinal must remain in the binding pocket of the protein because in the seconds timescale it is rebound, and restores the ground-state pHR, capable for the further photocycle.

The National Science Research Fund of Hungary OTKA T034788 and National Institutes of Health grant GM29498 (to J.K.L.) supported this work.

REFERENCES

Alshuth, T., M. Stockburger, P. Hegemann, and D. Oesterhelt. 1985. Structure of the retinal chromophore in halorhodopsin. A resonance Raman study. *FEBS Lett.* 179:55–59.

Ames, J. B., J. Raap, J. Lugtenburg, and R. A. Mathies. 1992. Resonance Raman study of halorhodopsin photocycle kinetics, chromophore structure, and chloride-pumping mechanism. *Biochemistry.* 31:12546–12554.

Balashov, S. P., R. Govindjee, M. Kono, E. P. Lukashev, T. G. Ebrey, Y. Feng, R. K. Crouch, and D. R. Menick. 1992. Arg82ala mutant of bacteriorhodopsin expressed in H. halobium: drastic decrease in the rate of proton release and effect on dark adaptation. *In* Structures and Functions of Retinal Proteins. J. L. Rigaud, editor. John Libbey Eurotext, Montrouge, France. 111–114.

Bamberg, E., P. Hegemann, and D. Oesterhelt. 1984. Reconstitution of the light-driven electrogenic ion pump halorhodopsin into black lipid membranes. *Biochim. Biophys. Acta.* 773:53–60.

Bamberg, E., D. Oesterhelt, and J. Tittor. 1994. Function of halorhodopsin as a light-driven H^+ pump. *Ren. Physiol. Biochem.* 17:194–197.

Bamberg, E., J. Tittor, and D. Oesterhelt. 1993. Light-driven proton or chloride pumping by halorhodopsin. *Proc. Natl. Acad. Sci. USA.* 90:639–643.

Bivin, D. B., and W. Stoeckenius. 1986. Photoactive retinal pigments in haloalkalophilic bacteria. *J. Gen. Microbiol.* 132:2167–2177.

Blanck, A., and D. Oesterhelt. 1987. The halorhodopsin gene II. Sequence, primary structure of halorhodopsin, and comparison with bacteriorhodopsin. *EMBO J.* 6:265–273.

Braiman, M. S., T. J. Walter, and D. M. Briercheck. 1994. Infrared spectroscopic detection of light-induced change in chloride-arginine interaction in halorhodopsin. *Biochemistry.* 33:1629–1635.

Cao, Y., G. Váró, A. L. Klinger, D. M. Czajkowsky, M. S. Braiman, R. Needleman, and J. K. Lanyi. 1993. Proton transfer from asp-96 to the bacteriorhodopsin Schiff base is caused by decrease of the pKa of asp-96 which follows a protein backbone conformation change. *Biochemistry.* 32:1981–1990.

Chizhov, I., and M. Engelhard. 2001. Temperature and halide dependence of the photocycle of halorhodopsin from *Natronobacterium pharaonis*. *Biophys. J.* 81:1600–1612.

Dér, A., K. Fendler, L. Keszthelyi, and E. Bamberg. 1985a. Primary charge separation in halorhodopsin. *FEBS Lett.* 187:233–236.

Dér, A., P. Hargittai, and J. Simon. 1985b. Time-resolved photoelectric and absorption signals from oriented purple membranes immobilized in gel. *J. Biochem. Biophys. Methods.* 10:295–300.

Duschl, A., J. K. Lanyi, and L. Zimányi. 1990. Properties and photochemistry of a halorhodopsin from the haloalkalophile, Natronobacterium pharaonis. *J. Biol. Chem.* 265:1261–1267.

Facciotti, M. T., V. S. Cheung, D. Nguyen, S. Rouhani, and R. M. Glaeser. 2003. Crystal structure of the bromide-bound D85S mutant of bacteriorhodopsin: Principles of ion pumping. *Biophys. J.* 85:451–458.

Fisher, M. M., and K. Weiss. 1974. Laser photolysis of retinal and its protonated and unprotonated n-butylamine Schiff base. *Photochem. Photobiol.* 20:423–432.

Gergely, C., L. Zimányi, and G. Váró. 1997. Bacteriorhodopsin intermediate spectra determined over a wide pH range. *J. Phys. Chem. B.* 101:9390–9395.

Gerscher, S., M. Mylrajan, P. Hildebrandt, M. H. Baron, R. Müller, and M. Engelhard. 1997. Chromophore-anion interactions in halorhodopsin from *Natronobacterium pharaonis* probed by time-resolved resonance Raman spectroscopy. *Biochemistry.* 36:11012–11020.

Golub, G., and W. Kahan. 1992. Calculating the singular values and pseudo-inverse of a matrix. *SIAM J. Numer. Anal.* 2:205–224.

Hackmann, C., J. Guijarro, I. Chizhov, M. Engelhard, C. Rodig, and F. Siebert. 2001. Static and time-resolved step-scan Fourier transform infrared investigations of the photoreaction of halorhodopsin from *Natronobacterium pharaonis*: Consequences for models of the anion translocation mechanism. *Biophys. J.* 81:394–406.

Havelka, W. A., R. Henderson, and D. Oesterhelt. 1995. Three-dimensional structure of halorhodopsin at 7 Å resolution. *J. Mol. Biol.* 247:726–738.

Hegemann, P., D. Oesterhelt, and M. Steiner. 1985. The photocycle of the chloride pump halorhodopsin. I. Azide catalyzed deprotonation of the chromophore is a side reaction of photocycle intermediates inactivating the pump. *EMBO J.* 4:2347–2350.

Kalaidzidis, I. V., Y. L. Kalaidzidis, and A. D. Kaulen. 1998. Flash-induced voltage changes in halorhodopsin from *Natronobacterium pharaonis*. *FEBS Lett.* 427:59–63.

Kolbe, M., H. Besir, L. O. Essen, and D. Oesterhelt. 2000. Structure of the light-driven chloride pump halorhodopsin at 1.8 Å resolution. *Science.* 288:1390–1396.

Lakatos, M., J. K. Lanyi, J. Szakács, and G. Váró. 2003. The photochemical reaction cycle of proteorhodopsin at low pH. *Biophys. J.* 84:3252–3256.

Lanyi, J. K., A. Duschl, G. W. Hatfield, K. M. May, and D. Oesterhelt. 1990. The primary structure of a halorhodopsin from Natronobacterium

pharaonis: structural, functional and evolutionary implications for bacterial rhodopsins and halorhodopsins. *J. Biol. Chem.* 265:1253–1260.

Lindley, E. V., and R. E. MacDonald. 1979. A second mechanism for sodium extrusion in Halobacterium halobium: A light-driven sodium pump. *Biochem. Biophys. Res. Commun.* 88:491–499.

Ludmann, K., C. Gergely, A. Dér, and G. Váró. 1998b. Electric signals during the bacteriorhodopsin photocycle, determined over a wide pH range. *Biophys. J.* 75:3120–3126.

Ludmann, K., C. Gergely, and G. Váró. 1998a. Kinetic and thermodynamic study of the bacteriorhodopsin photocycle over a wide pH range. *Biophys. J.* 75:3110–3119.

Ludmann, K., G. Ibron, J. K. Lanyi, and G. Váró. 2000. Charge motions during the photcycle of *pharaonis* halorhodopsin. *Biophys. J.* 78:959–966.

Maeda, A., T. Ogurusu, T. Yoshizawa, and T. Kitagawa. 1985. Resonance Raman study on binding of chloride to the chromophore of halorhodopsin. *Biochemistry.* 24:2517–2521.

Matsuno-Yagi, A., and Y. Mukohata. 1977. Two possible roles of bacteriorhodopsin: A comparative study of strains of Halobacterium halobium differing in pigmentation. *Biochem. Biophys. Res. Commun.* 78:237–243.

Mukohata, Y., K. Ihara, T. Tamura, and Y. Sugiyama. 1999. Halobacterial rhodopsins. *J. Biochem. (Tokyo).* 125:649–657.

Muneyuki, E., C. Shibazaki, Y. Wada, M. Yakushizin, and H. Ohtani. 2002. Cl^- concentration dependence of photovoltage generation by halorhodopsin from *Halobacterium salinarum*. *Biophys. J.* 83:1749–1759.

Needleman, R., M. Chang, B. Ni, G. Váró, J. Fornes, S. H. White, and J. K. Lanyi. 1991. Properties of asp212-asn bacteriorhodopsin suggest that asp212 and asp85 both participate in a counterion and proton acceptor complex near the Schiff base. *J. Biol. Chem.* 266:11478–11484.

Oesterhelt, D., P. Hegemann, P. Tavan, and K. Schulten. 1986. Trans-cis isomerization of retinal and a mechanism for ion translocation in halorhodopsin. *Eur. Biophys. J.* 14:123–129.

Okuno, D., M. Asaumi, and E. Muneyuki. 1999. Chloride concentration dependency of the electrogenic activity of halorhodopsin. *Biochemistry.* 38:5422–5429.

Otomo, J., H. Tomioka, and H. Sasabe. 1992. Properties and the primary structure of a new halorhodopsin from halobacterial strain mex. *Biochim. Biophys. Acta.* 1112:7–13.

Pande, C., J. K. Lanyi, and R. H. Callender. 1989. Effects of various anions on the Raman spectrum of halorhodopsin. *Biophys. J.* 55:425–431.

Rothschild, K. J., O. Bousché, M. S. Braiman, C. A. Hasselbacher, and J. L. Spudich. 1988. Fourier transform infrared study of the halorhodopsin chloride pump. *Biochemistry.* 27:2420–2424.

Scharf, B., and M. Engelhard. 1994. Blue halorhodopsin from *Natronobacterium pharaonis*: Wavelength regulation by anions. *Biochemistry.* 33:6387–6393.

Schobert, B., and J. K. Lanyi. 1982. Halorhodopsin is a light-driven chloride pump. *J. Biol. Chem.* 257:10306–10313.

Soppa, J., J. Duschl, and D. Oesterhelt. 1993. Bacterioopsin, haloopsin, and sensory opsin I of the halobacterial isolate *Halobacterium* sp. strain SG1: Three new members of a growing family. *J. Bacteriol.* 175:2720–2726.

Stoeckenius, W., R. H. Lozier, and R. A. Bogomolni. 1979. Bacteriorhodopsin and the purple membrane of halobacteria. *Biochim. Biophys. Acta.* 505:215–278.

Váró, G., L. S. Brown, M. Lakatos, and J. K. Lanyi. 2003. Characterization of the photochemical reaction cycle of proteorhodopsin. *Biophys. J.* 84: 1202–1207.

Váró, G., L. S. Brown, R. Needleman, and J. K. Lanyi. 1996. Proton transport by Halorhodopsin. *Biochemistry.* 35:6604–6611.

Váró, G., L. S. Brown, N. Sasaki, H. Kandori, A. Maeda, R. Needleman, and J. K. Lanyi. 1995b. Light-driven chloride ion transport by Halorhodopsin from *Natronobacterium pharaonis*. 1. The photochemical cycle. *Biochemistry.* 34:14490–14499.

Váró, G., R. Needleman, and J. K. Lanyi. 1995a. Light-driven chloride ion transport by Halorhodopsin from *Natronobacterium pharaonis*. 2. Chloride release and uptake, protein conformation change, and thermodynamics. *Biochemistry.* 34:14500–14507.

Váró, G., L. Zimányi, X. Fan, L. Sun, R. Needleman, and J. K. Lanyi. 1995c. Photocycle of halorhodopsin from *Halobacterium salinarium*. *Biophys. J.* 68:2062–2072.

Zimányi, L., L. Keszthelyi, and J. K. Lanyi. 1989. Transient spectroscopy of bacterial rhodopsins with optical multichannel analyser. 1. Comparison of the photocycles of bacteriorhodopsin and halorhodopsin. *Biochemistry.* 28:5165–5172.

Zimányi, L., and J. K. Lanyi. 1989. Transient spectroscopy of bacterial rhodopsins with optical multichannel analyzer. 2. Effects of anions on the halorhodopsin photocycle. *Biochemistry.* 28:5172–5178.

Zimányi, L., and J. K. Lanyi. 1997. Fourier transform Raman study of retinal isomeric composition and equilibration in halorhodopsin. *J. Phys. Chem. B.* 101:1930–1933.